Separation and Purification Technology 305 (2023) 122563

Contents lists available at ScienceDirect

Separation and Purification Technology

journal homepage: www.elsevier.com/locate/seppur

Inactivation of ciliate *Uronema marinum* under UV/peroxydisulfate advanced disinfection system in marine water

Yuanyuan Zhang [a,b], Kunling Huang [a], Xuan Chen [a], Min Wei [a], Xiaopeng Yu [a], Hongfei Su [a], Pin Gan [a], Kefu Yu [a,b,*]

[a] School of Marine Sciences, Guangxi Laboratory on the Study of Coral Reefs in the South China Sea, Guangxi University, Nanning 530004, China
[b] Southern Marine Science and Engineering Guangdong Laboratory (Zhuhai), Zhuhai 519000, China

ARTICLE INFO

Keywords:
Protozoa
Uronema marinum
Inactivation
UV/PDS
Sulfate radical

ABSTRACT

Protozoa in mariculture water will cause the outbreak of seafood diseases, and there are also discharge regulations about protozoa in the ballast water of ocean ships. However, the inactivation of protozoa has not attracted attention. This study investigated the inactivation of ciliate *Uronema marinum* (*U. marinum*) as surrogate for protozoa by ultraviolet (UV)/peroxydisulfate (PDS) system. Results showed that the addition of 1 mM PDS significantly enhanced the inactivation from 0.73 log to 1.47 log by UV exposure at 3.6 mJ·cm^{-2}. Reactive species responsible for the inactivation were identified to be $\bullet SO_4^-$ and •OH. The anions in seawater inhibited the inactivation of *U. marinum* in UV/PDS system. UV/PDS inactivated *U. marinum* by damaging the cell membrane and releasing of intracellular materials. The activities change of the antioxidant enzymes showed that oxidative species destroyed the defense function. Moreover, omics analysis proved that the radicals affected the expression of genes, proteins and metabolites of *U.marinum*. In authentic marine water, the inactivation of *U. marinum* was 1.38 log in 120 s. There was no generation of chlorate (ClO_3^-), bromate (BrO_3^-) and adsorbable organic halogens (AOX). The economic cost of UV/PDS for inactivation of *U. marinum* was preliminarily calculated to be 0.062 $ m^{-3}. The results suggest that it will be beneficial to upgrade UV disinfection to $\bullet SO_4^-$ based advanced oxidation technology for inactivation of protozoa in marine water.

1. Introduction

Generally, people pay much attention to the disinfection of drinking water and wastewater such as medical sewage, the existence of harmful organisms in marine water should not be ignored [1–4]. Recently, some studies have reported the inactivation of microalgae, bacteria and virus in marine water, etc [5–7]. However, few researches were focused on the inactivation of marine protozoa. The outbreak of pathogenic protozoa in marine aquaculture water caused serious infectious diseases. For example, ciliate *Uronema marinum* (*U. marinum*), a common unicellular organism which lived freely in marine aquaculture water was the causative agent of scuticociliatosis in farm raised turbot *Scophthalmus maximus* [8]. *Cryptosporidium* and *Giardia* are common protozoan parasites which can cause severe diseases and even death in immune deficient hosts. *Toxoplasma gondii* can cause toxoplasmosis, it is pathogenic to humans and animals [9]. The discharge of ballast water from the vessel leads to transoceanic movement of indigenous marine protozoa, which can cause serious environmental problems. As regulated by the ballast water discharge standard of "International Maritime Organization (IMO)", there should be no more than 10 organisms per milliliter with body length of 10–50 μm which range are consistent with many species of marine protozoa [10]. The size of protozoa generally ranges from a few microns to tens of microns, which belongs to the range specified in the standard. Therefore, it is necessary to develop a disinfection system for marine water that can inactivate protozoa effectively.

The traditional disinfection methods include chlorination, ultraviolet (UV) irradiation and ozone oxidation, etc [11–13]. While eliminating pathogens, chlorine containing disinfectants can react with organic substances to generate harmful halogenated disinfection by-products (DBPs) [14–16]. The disinfection efficiencies of UV irradiation are not satisfactory [17]. Bromate with high carcinogenic possibility will be formed during ozone disinfection of water containing bromine [18,19]. Advanced oxidation technologies (AOTs) which produced reactive hydroxyl radical (•OH) have been widely used in water disinfection

* Corresponding author.
E-mail address: kefuyu@scsio.ac.cn (K. Yu).

https://doi.org/10.1016/j.seppur.2022.122563
Received 5 August 2022; Received in revised form 26 October 2022; Accepted 1 November 2022
Available online 5 November 2022

[20–22]. The redox potential of $\bullet SO_4^-$ (i.e., $E^0 = 2.5–3.1$ V) is higher than •OH (i.e., $E^0 = 1.8–2.7$ V), and the half-life of $\bullet SO_4^-$ (30–40 μs) is longer than that of •OH (less than 1 μs). In addition, $\bullet SO_4^-$ has a higher selectivity for electron-rich chemicals on macromolecules/biomolecules compared to •OH [23]. Therefore, $\bullet SO_4^-$ based AOTs including peroxydisulfate ($S_2O_8^{2-}$, PDS) and peroxymonosulfate (HSO_5^-, PMS) activation have recently been employed for water disinfection and proved to be efficient and environmentally friendly [24–26]. Most of these studies have focused on the degradation of organic pollutants by PDS/PMS activation [27–29]. In recent years, the research on microorganism inactivation is getting more and more attention. For example, Michael-Kordatou et al. upgraded the experimental conditions from UV to UV/PDS, the inactivation time of total *Escherichia coli* (*E.coli*) and erythromycin resistant *E.coli* decreased significantly from 45 min and 90 min to 30 min and 45 min, respectively [30]. Sun et al. examined the inactivation of *Escherichia coli*, bacteriophage *MS2*, and *Bacillus subtilis spores* under UV/H_2O_2 and UV/PDS conditions. The study found that different species had different outcomes of inactivation efficiency under the same treatment [31]. This may be due to particular disinfection mechanisms between specific microorganisms and radicals. Moreover, the anions in marine water may react with $\bullet SO_4^-$ to produce oxidation species such as reactive chlorine species (RCs) which may also effective for microorganism inactivation [32–34]. Many studies have reported that AOTs can effectively inactivate algae and bacteria in ship's ballast water. For example, Bai et al. found that the •OH can rapidly inactivate algae and bacteria by destroying their cellular membrane, which achieved D-2 ballast water discharge standard of IMO [35]. Moreno-Andres et al. reported that free radicals generated by an electrochemical AOT can effectively inactivate marine heterotrophic bacteria in ballast water [36]. However, to the best of our knowledge, UV/PDS has not been investigated for the inactivation of protozoa in marine water.

On the other hand, only a few relevant reports have pointed out that when microorganisms were exposed to an environment rich in $\bullet SO_4^-$, their cell membrane/wall, genetic material DNA/RNA and enzyme activities may be damaged [17,37–39]. In recent years, with the rapid development of high-throughput sequencing technology, omics including transcriptomics, proteomics and metabolomics were widely used in various research fields [40–42]. However, the study on the mechanism of $\bullet SO_4^-$ inactivation of organisms by multi-omics has neither been reported. Thus, it is imperative to investigate the efficiency of UV/PDS in inactivating protozoa in marine water and the mechanisms based on omics.

This study employed ciliate *U. marinum* as a representative of protozoa in marine water. The inactivation dynamic kinetics of *U. marinum* under various treatment conditions, formation of radicals in UV/PDS system and their contributions to inactivation were investigated. The reaction parameters were optimized to guide the practical application in marine water disinfection. The overall response of biological cells was analyzed from the changes of cell integrity and enzyme activity, combined with transcriptomics, proteomics and metabolomics to clarify the mechanism of biological inactivation. In addition, the formation of disinfection by-products (DBPs) including ClO_3^-, BrO_3^- and AOX were checked to confirm the application feasibility of UV/PDS on marine water disinfection.

2. Materials and methods

2.1. Chemicals.

Sources of chemical and reagents are provided in the Supporting Information (SI) Text S1.

2.2. Marine ciliate

U. marinum was purchased from Institute of Hydrobiology, Chinese Academy of Sciences. Details of *U. marinum* are described in SI Text S2 and Fig.S1. Clonal cultures were established by laboratory. A single cell was isolated from the original population by pipette. Then it was washed several times in steriled seawater to decrease the presence of contaminating microorganisms. The clean single cell was cultured in petrie dish with nutrient, which was counted every 24 h until the cells were around 100. To expand the culture, the ciliates in the petri dish were transferred to the flask with the nutrient. Cliate *U. marinum* was incubated at 22 ~ 25 °C for expansion (water temperature 20–25 °C; salinity 35 ‰; pH 8). Bacterial were the food source for the ciliated protozoa. The grain was naturally grown bacterial feed. Add 10 wheat grains to 100 mL of sterilized seawater and incubate at 37 °C for 24 h to obtain a wheat grain extract, which is used as a nutrient source [43].

2.3. Experimental procedures

The inactivation experiments were conducted with a reactor equipped with a collimated-beam UV apparatus and a quartz reaction tube (2.5 cm diameter, 18 cm length) in Fig.S2. A low-pressure mercury lamp emitting light predominantly at 254 nm was used as the light source. Details about incident fluence rate measurement were shown in SI Text S3 and Fig.S3. The ciliate suspension (20 mL) was put into quartz reaction tube which was placed on a stir plate, parallel to the incident light. Most of the experiments were conducted in sterilized seawater (35 ‰) containing 1 mM PDS, 14 W UV, and 3000 cells·mL^{-1} initial density, except where stated otherwise. In the kinetics studies, the effects on inactivation of PDS concentration (0.01, 0.1, 1 mM), UV intensity (6, 14, 25 W), initial ciliate concentration (3000, 5000, 10,000 cells·mL^{-1}), DOC concentration (15, 20, 30 mg·L^{-1}) and salinity of sea water (12, 17, 35 ‰) were checked. Free radicals were quenched by methanol (1 mM) and *tert*-butyl alcohol (TBA) (1 mM). The steady-state concentrations of $\bullet SO_4^-$, •OH, •Cl, •ClO can be determined by adding four probes, 5 μM nitrobenzene (NB), 5 μM anisole (AS), 5 μM benzoic acid (BA) and 5 μM 1,4-dimethoxybenzene (DMOB) to the UV/PDS system (details shown in SI Text S4) [44,45].

At different time intervals, aliquot samples (1 mL) were collected. Then cells were measured by micro-counting method under the biological microscope [46]. To ensure the reproducibility of the average values, all experiments were conducted in triplicate. Inactivation efficiencies were calculated by Eq. (1), N_0 and N_t are concentrations of ciliate *U. marinum* in the untreated water sample and the equivalent water sample after inactivation, respectively. The kinetic rate constant *k* was then calculated by linear relation between $\log(N_0/N_t)$ and UV irradiation time *t* as described by Sun et al [31].

$$S = \log\left(\frac{N_0}{N_t}\right) \quad (1)$$

$$\log\left(\frac{N_0}{N_t}\right) = kt \quad (2)$$

2.4. Disinfection mechanisms experiments

The appearances of *U. marinum* were observed by scanning electron microscopy (SEM) (FEI Quattro S). Detailed operation steps are shown in SI Text S5. *U. marinum* suspension was centrifuged for 10 min at 8,000 rpm, then the concentration of the extracellular DNA was determined by the absorbance of supernatant with a microplate reader at wavelengths of 260 nm (A260) and 280 nm (A280) [17]. The intracellular enzyme protein was extracted using bicinchoninic acid (BCA) method, superoxide dismutase (SOD) and catalase (CAT) activities were measured by the WST-8 and ammonium molybdate method, respectively [37,47,48].

In transcriptomics analysis, total RNA was extracted from samples with Trizol reagent kit (Invitrogen, Carlsbad, CA, USA). The quality of RNA was estimated, then the enriched mRNA was fragmented and reverse transcribed into cDNA using random primers. The constructed library was sequenced using an Illumina novaseq 6000. Functional

analysis of the differentially expressed genes was performed using the KEGG database. For details, see in SI Text S6. In proteomics analysis, sample was prepared with iST Sample Preparation kit (Pre-Omics, Germany). The peptide mixture was fractionated by high pH separation using Ultimate 3000 system (Thermo Fisher scientific, MA, USA), and further analyzed by on-line nanospray LC-MS/MS. Differentially expressed proteins were further annotated against KEGG databases to determine their functions. For details, see in SI Text S7. In metabolomics analysis, the samples were prepared, which was injected into the LC-MS/MS system analysis. The samples were analyzed using a Vanquish UHPLC system (Thermo Fisher, Germany). The raw data files were processed using the Compound Discoverer 3.1 (CD3.1, Thermo Fisher). Pathway enrichment analysis was performed using the Metabo Analyst and DAVID toolkits. For details, see in SI Text S8.

2.5. Disinfection by-products experiments

Humic acid (0.01, 0.1, 1, mM) was added to the simulated marine water. ClO_3^- and BrO_3^- which were measured by using ion chromatography (ICS-900, Thermo Fisher Scientific), the effluent was a mixture of 4.5 mM sodium carbonate and 0.8 mM sodium bicarbonate at a flow rate of 0.30 mL min^{-1}. Meanwhile, adsorbable organic halogen (AOX) was determined by a total organic halogen analyzer (XPLORER, TE instruments) [49,50]. The toxicity of the UV/PDS reaction system was studied by the growth inhibition of *U. marinum*. 1 mL of 10^3 cells·mL^{-1} of *U. marinum* were added to the reaction solutions, Then the *U. marinum* were incubated at 37 °C for 24 h to calculate the total number of cells.

3. Results and discussion

3.1. Inactivation of ciliate U. marinum by UV, PDS and UV/PDS

U. marinum was treated under UV, PDS and UV/PDS conditions (Fig. 1). The results showed that *U. marinum* was not inactivated by PDS alone within 120 s. The inactivation by UV irradiation alone presented a lag phase during the initial phase for around 1.35 mJ·cm^{-2} and followed by a linear increase along with the exposure time. 0.73 log inactivation of *U. marinum* was finally achieved by UV exposure at 3.6 mJ·cm^{-2}. The phenomenon was similar to the UV inactivation of *E. coli* and *Bacillus subtilis* spores reported by Sun et al [31]. The platform in the initial stage under UV irradiation may be due to the resurrection process, the same as the research on inactivation of *feline calicivirus* [51]. It has been proved

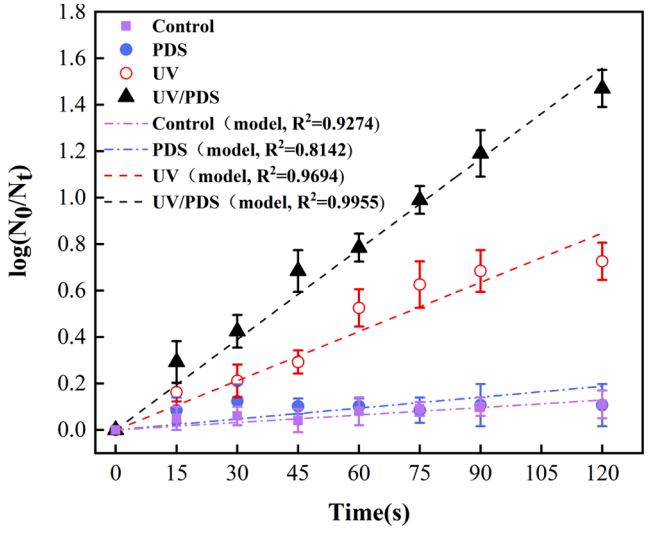

Fig. 1. Inactivation of *U. marinum* under UV, PDS and UV/PDS conditions. (*U. marinum* = 3000 cells·mL^{-1}, PDS = 1 mM, Light power = 14 W, T = 298.15 K, pH = 8).

that the inactivation of microorganisms by UV irradiation was mainly due to the damage to the nucleic acids of the cell [52]. The limited inactivation effect may be attributed to the repair mechanisms developed by microorganisms [53].

The addition of 1 mM PDS significantly enhanced the inactivation of *U. marinum*. The initial inactivation lag phase under UV treatment alone disappeared and replaced by a continuous loss of protozoan viability. Under UV/PDS treatment, 1.47 log inactivation was achieved at 3.6 mJ·cm^{-2}. The kinetic rate constant *k* also increased from 0.0071 s^{-1} to 0.0130 s^{-1}. The radical attack may be primarily responsible for the continuous and rapid inactivation of *U. marinum* because the reactive species such as $\bullet SO_4^-$ and •OH should be formed through the following ways in UV/PDS system (Eq.3–4). Considering the the complex composition of authentic marine water matrix, inactivation experiments of *U. marinum* in authentic water were studied. As shown in Fig.S4, the dynamic kinetics of *U. marinum* inactivation in the authentic marine water showed similar trend in the synthetic marine water. The inactivation of *U. marinum* was 1.47 log and 1.38 log in the simulated and authentic marine water bodies at 120 s, respectively. The slight decrease of inactivation efficiency may be due to the competitive oxidation of organic matter in the authentic marine water. The results showed that the synthetic marine water matrix prepared on the basis of marine water components can well simulate the authentic marine water matrix, and the research conducted in the synthetic marine water matrix can represent the *U. marinum* inactivation in the authentic marine water matrix. Further studies were conducted to identify the contribution of the reactive radicals on the inactivation of *U. marinum*.

$$S_2O_8^{2-} + h\nu \rightarrow 2\cdot SO_4^- \quad (3)$$

$$\cdot SO_4^- + OH^- \rightarrow \cdot OH + SO_4^{2-} \quad (4)$$

3.2. Contribution of reactive species on the inactivation of U. marinum

The activation of PDS by UV irradiation produces primary radicals including $\bullet SO_4^-$ and •OH. The primary radicals in marine water under UV/PDS treatment were first identified by ESR spectroscopy. Dimethyl-1-pyrroline *N*-oxide (DMPO) was applied to demonstrate the formation of $\bullet SO_4^-$ and •OH [37]. As shown in Fig.S5, the radical adducts signals of DMPO-$\bullet SO_4^-$ and DMPO-•OH proved that these two primary radicals were coexisting in the UV/PDS treatment of marine water [54].

Steady-state concentration of free radicals were measured by radical probes. As shown in Fig. 2A, the concentration of sulfate radical was 1.07×10^{-13} M, and the concentration of hydroxyl radical was 2.73×10^{-14} M which is 3.9 times that of sulfate radical. Each radical has a different reaction rates, therefore we analyzed the contributions of radicals on the inactivation of *U. marinum* by adding radical scavengers. Preliminary experiments were conducted to confirm that these two radical scavengers did not show detectable impact on *U. marinum*. As shown in Fig. 2B, the inactivation of *U. marinum* treated by UV, UV/PDS and UV/PDS + methanol system was 0.73 log, 1.47 log and 0.88 log in 120 s, respectively. The difference of 0.74 log between UV and UV/PDS should be due to the inactivation contribution of reactive oxidizing species. The difference of 0.59 log between UV/PDS + methanol and UV/PDS should be due to the inactivation contribution of $\bullet SO_4^-$ and •OH as it is well known that methanol can effectively scavenge both these two radicals [30,37]. The inactivation contribution rate of $\bullet SO_4^-$ and •OH accounted for 80 % of all reactive oxidizing species. It was reported that TBA could quench for •OH effectively, but not for $\bullet SO_4^-$, RCs and carbonate radicals [55]. The inactivation of *U. marinum* in UV/PDS + TBA system was 1.19 log in 120 s and then the inactivation contribution of •OH was calculated to be 0.28 log. Therefore, the inactivation contribution of $\bullet SO_4^-$ was calculated as 0.31 log. The contribution of $\bullet SO_4^-$ was slightly higher than •OH, which is consistent with the radical concentration results.

Secondary radicals such as RCs and carbonate radicals will be formed

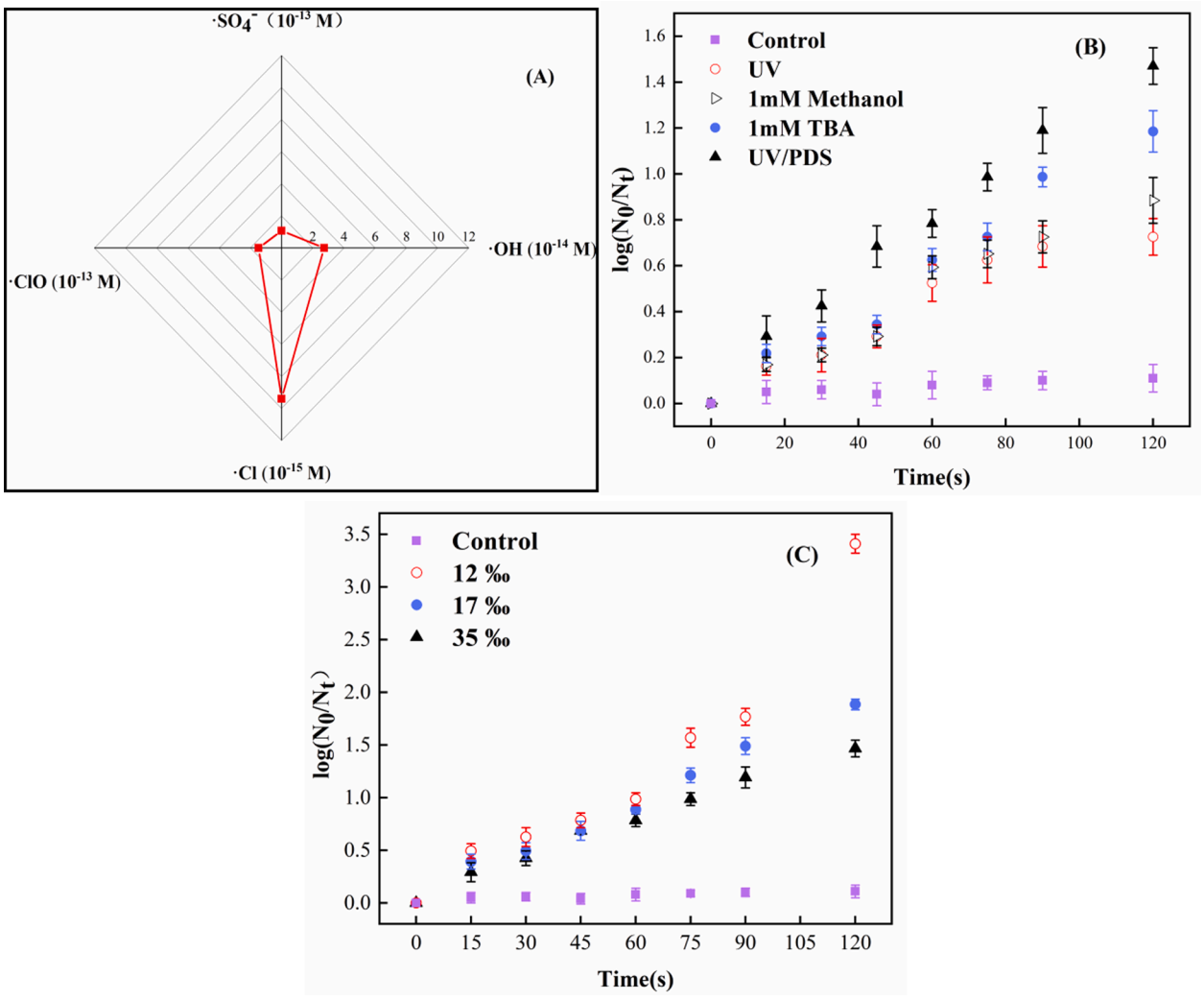

Fig. 2. Contributions of reactive species generated in UV/PDS systems. **(A)** Molar Concentrations of Reactive Species. **(B)** Inactivation of *U. marinum* in the presence of methanol or TBA as radical scavenger; **(C)** Inactivation of *U. marinum* under different salinity. (*U. marinum* = 3000 cells·mL^{-1}, PDS = 1 mM, Methanol = 1 mM, ert-Butyl alcohol = 1 mM, Light power = 14 W, T = 298.15 K, pH = 8).

by the reaction of •SO_4^- and •OH with marine water anions as follows (Eq.5–16) [56–59]. The inactivation contribution of anions were then evaluated by changing the salinity within a reasonable range which was confirmed to have negligible impact on *U. marinum* previously. The concentration of anions in the seawater are summarized in SI Table S1. As shown in Fig. 2C, the inactivation increased from 1.47 log to 1.88 log and 3.41 log in 120 s when the salinity of sea water decreased from 35 ‰ to 17 ‰ and 12 ‰, respectively. The inactivation significantly decreased with the increase of salinity, indicating that the anions in seawater inhibited the inactivation of *U. marinum* in UV/PDS system. Similar inhibitory effects have also been reported on UV/PDS inactivation of *E. coli* and *Streptococcus agalactiae* [49]. The reason should be attributed to that the reaction of anions with radicals, and then the amount of effective •SO_4^- in the UV/PDS system was reduced. Although secondary radicals can inactivate microorganisms, they have oxidation capacities that are relatively weaker than that of •SO_4^-. In UV/PDS, the concentration of •Cl and •ClO were 9.40 × 10^{-15} M and 1.47 × 10^{-13} M (Fig. 2A), respectively, but chloride ion in seawater inhibited the inactivation of *U. marinum*, so we speculate *U. marinum* may be insensitive to •Cl and •ClO. The above results showed that *U. marinum* were mainly inactivated by the primary radicals including •SO_4^- and •OH in the UV/PDS system in marine water.

$$\cdot SO_4^- + Cl^- \rightarrow SO_4^{2-} + \cdot Cl \quad k = 2.7 \times 108M^{-1}S^{-1} \quad (5)$$

$$\cdot Cl + Cl^- \rightarrow \cdot Cl_2^- \quad k = 8 \times 10^9 M^{-1}S^{-1} \quad (6)$$

$$\cdot Cl_2^- + \cdot Cl_2^- \rightarrow 2Cl^- + Cl_2 \quad k = 2.1 \times 10^9 M^{-1}S^{-1} \quad (7)$$

$$\cdot Cl_2^- + \cdot OH \rightarrow Cl^- + HClO \quad k = 1.0 \times 10^9 M^{-1}S^{-1} \quad (8)$$

$$Cl^- \xrightarrow{\cdot SO_4^-,\cdot OH} HClO/ClO^- \xrightarrow{\cdot SO_4^-,\cdot OH} ClO_3^- \quad (9)$$

$$\cdot SO_4^- + Br^- \rightarrow SO_4^{2-} + \cdot Br \quad k = 3.5 \times 1010M - 1S - 1 \quad (10)$$

$$\cdot Br + Br^- \rightarrow \cdot Br_2^- \quad k = 1.2 \times 10^{10} M^{-1}S^{-1} \quad (11)$$

$$Br^- \xrightarrow{\cdot SO_4^-,\cdot OH} HBrO/BrO^- \xrightarrow{\cdot SO_4^-,\cdot OH} BrO_3^- \quad (12)$$

$$\cdot SO_4^- + HCO_3^- \rightarrow \cdot HCO_3 + SO_4^{2-} \quad k = 1.6 \times 10^6 M^{-1}S^{-1} \quad (13)$$

$$HCO_3^- + \cdot OH \rightarrow \cdot CO_3^- + H_2O \quad k = 8.5 \times 106M - 1S - 1 \quad (14)$$

$$\cdot SO_4^- + \cdot OH \rightarrow HSO_5^- \quad k = 1.0 \times 10^{10} M^{-1}S^{-1} \quad (15)$$

$$\cdot SO_4^- + SO_4^{2-} \rightarrow S_2O_8^{2-} + e_{aq}^- \quad (16)$$

concentrations of radicals.

3.3. Effect of reaction parameters on the inactivation of *U. marinum*

Different intensities of UV light and concentrations of PDS were first employed to evaluate the influence of the operating parameters on *U. marinum* inactivation. As shown in Fig. 3(A), the inactivation increased from 0.47 log to 3.25 log when the intensity of UV light was increased from 6 W to 25 W. The inactivation for 14 W was 1.47 log, 3.1 times as much as that for 6 W. However, the inactivation difference between 14 W and 25 W was just 2.2 times, much less than that between 6 W and 14 W. Therefore, the UV light with 14 W was chosen in other investigations to save energy. It can be seen from Fig. 3(B) that the inactivation of *U. marinum* by UV/PDS process was considerably dependent on the initial concentration of PDS. The single UV irradiation without PDS addition possessed certain inactivity towards *U. marinum*. The number slightly increased to 0.88 log and 1.00 log for PDS of 0.01 mM and 0.1 mM, respectively. For PDS of 1 mM, it reached 1.47 log and was 1.7 times as much as that for 0.01 mM. The results indicated that the more PDS, the more radicals generated by UV activation which played an important role in inactivation of *U. marinum*. However, it has been reported that a continuous increase of PDS after exceeding a certain amount could cause a decrease in the substrate removal in UV/PDS system [60,61]. The reason should be attributed to the quenching of the radicals by each other as well as the radical scavenging by $S_2O_8^{2-}$. The inhibition effect of PDS on *U. marinum* inactivation was not observed in this study because the highest PDS concentration of 1 mM may not reach the critical inhibition level that could quench the produced radicals and the phenomenon was similar with the oxidation of erythromycin by UV/PDS [30].

The effect of initial concentration of *U. marinum* on its inactivation was further examined in the UV/PDS system. As shown in Fig. 3(C), the inactivation decreased from 1.47 log to 1.39 log and 1.12 log when the concentration of *U. marinum* increased from 3000 cells·mL^{-1} to 5000 cells·mL^{-1} and 10,000 cells·mL^{-1} in 120 s, respectively. The result indicated that faster inactivation of *U. marinum* could be achieved at lower initial cell concentrations which was consistent with the photocatalytic inactivation of bacteria including *E. coli* and *Pichia Pastoris* [62]. The reason should be attributed to the proportion of reactive radicals was higher when the initial concentration of *U. marinum* was relatively lower, which provided a potential greater possibility for the inactivation of the ciliate [30].

The inactivation of *U. marinum* was also examined in marine water containing different concentrations of DOC synthetic. As shown in Fig. 3 (D), when the DOC concentration was 20 mg·L^{-1} (equivalent to the concentration in marine ballast water), the inactivation reached 1.47 log after 120 s treatment in UV/PDS system. The inactivation decreased to 0.88 log as the concentration of DOC increased to 30 mg·L^{-1} (equivalent to the concentration in marine aquaculture water). Reducing the DOC concentration to 15 mg·L^{-1} could increase the inactivation to 1.78 log. The results showed that the higher the concentration of DOC in marine water, the lower the inactivation of *U. marinum*. The coexisting DOC caused the competition for reactive radicals and reduced the amount of radicals acting on *U. marinum*. Nevertheless, in the DOC concentration

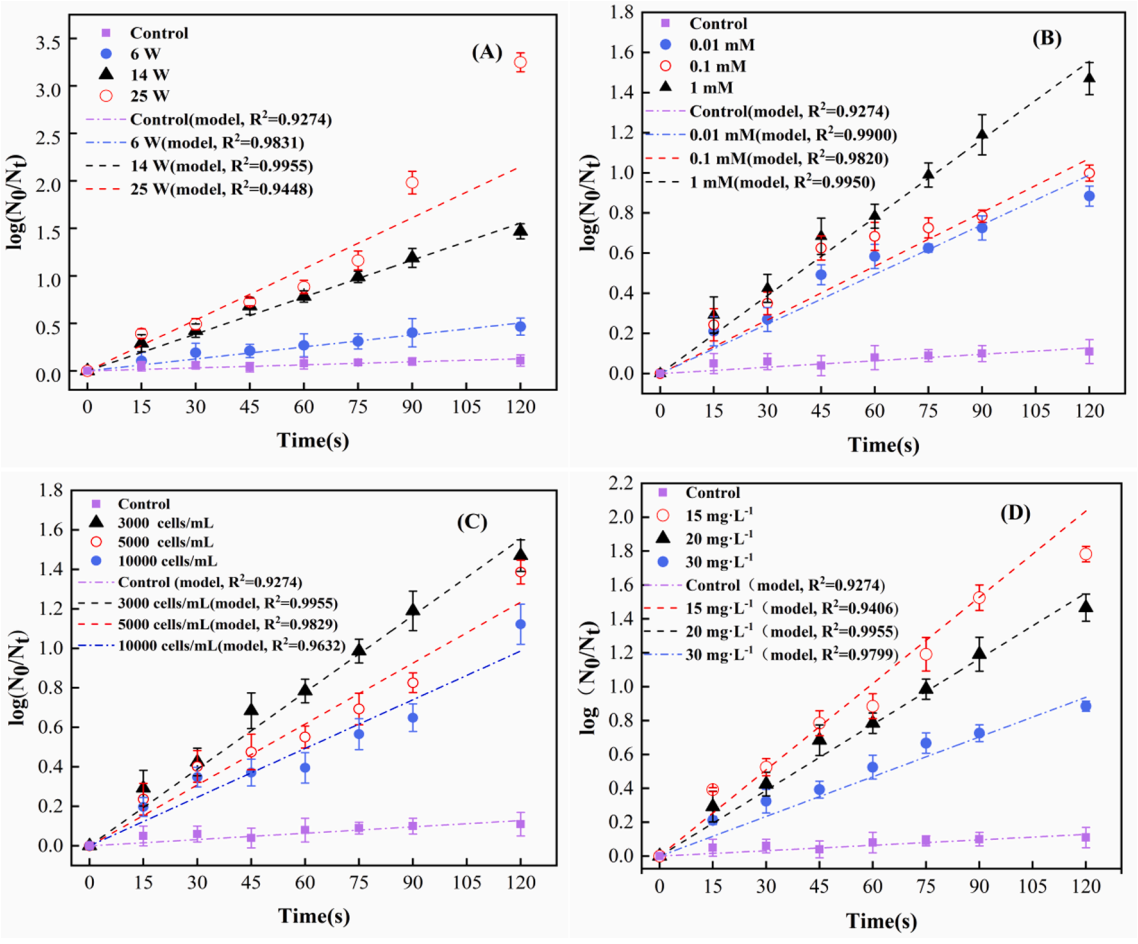

Fig. 3. Effect of reaction parameters on the inactivation of *U. marinum*. **(A)** UV light intensities (*U. marinum* = 3000 cells·mL^{-1}, PDS = 1 mM, DOC = 20 mg·L^{-1}, T = 298.15 K, pH = 8); **(B)** PDS concentrations (*U. marinum* = 3000 cells·mL^{-1}, DOC = 20 mg·L^{-1}, Light power = 14 W, T = 298.15 K, pH = 8); **(C)** initial cell concentration (PDS = 1 mM, DOC = 20 mg·L^{-1}, Light power = 14 W, T = 298.15 K, pH = 8); **(D)** initial concentration of DOC in marine water (*U. marinum* = 3000 cells·mL^{-1}, PDS = 1 mM, Light power = 14 W, T = 298.15 K, pH = 8).

range of marine ballast water and marine aquaculture water, UV/PDS system with the above experimental conditions can inactivate *U. marinum* effectively.

In addition to *U. marinum*, other kinds of marine organisms have also been proved to be effectively inactivated by UV/PDS. For example, our previous research already studied the inactivation of bacteria including *Escherichia coli* (*E. coli*) and *Streptococcus agalactiae* (*S. agalactiae*) [49]. PDS alone has slight inactivation effects on the marine organisms. The inactivation efficiency of UV radiation alone was significantly lower than that under the UV/PDS treatment. The inactivation of microorganisms were significantly increased when PDS was added to the UV system. The inactivation efficiency of *E. coli*, *S. agalactiae*, and *U. marinum* were 4.13 log, 4.74 log, and 1.47 log by UV/PDS treatment at 120 s, respectively (Fig.S6). The results showed that UV/PDS is an efficient technology for inactivating marine microorganisms.

3.4. Inactivation mechanisms

Microorganisms would be mainly inactivated via destruction of cell membrane, genetic materials, and enzymes when exposed to $\bullet SO_4^-$ [26]. The apparent integrity of *U. marinum* cells was first checked by SEM. As shown in Fig. 4(A), the untreated *U. marinum* cell exhibited intact membrane, the cell irradiated by UV for 120 min did not show obvious break (Fig. 4(B)). On the contrast, *U. marinum* cells were completely ruptured after UV/PDS treatment (Fig. 4(C)). The results were consistent with the literature reported by Zeng et al. [63], after the UV/PDS treatment, the cell wall of chlorine-resistant bacterial spores was severely damaged, leaving only small pieces of cell debris, some apparent materials were found to be released from the cells, which were probable to be amino acids and carbohydrates. To further confirm the damage of *U. marinum* cell, the concentrations of extracellular genetic material DNA of *U. marinum* after treated by UV, PDS and UV/PDS systems for 120 min were detected. Because the organisms would update regularly and release dead cells containing DNA, when various organisms interacted with the environment normally, DNA would be discharged and accumulated in their surroundings [17]. As shown in Fig. 5 the initial data of the test (2.66 ng·μL^{-1}) was the environmental DNA concentration. Within 120 min, there was no significant change in extracellular DNA concentration after PDS or UV treatment alone, however, after UV/PDS treatment, the concentration reached 7.35 ng·μL^{-1}. The results indicated that UV/PDS system inactivated *U. marinum* by damaging the cell membrane and release of intracellular materials to the bulk solution which was opposite to UV irradiation. The reason may be due to that $\bullet SO_4^-$ and •OH could induce oxidative lipid peroxidation in the cell membrane resulting in perturbed membrane permeability, inhibiting normal metabolism and even leading to the inactivation of cells.

In addition, the antioxidant enzyme protects against oxidative stress from the environment. SOD catalyzes the decomposition of $\bullet O_2^-$ to H_2O_2,

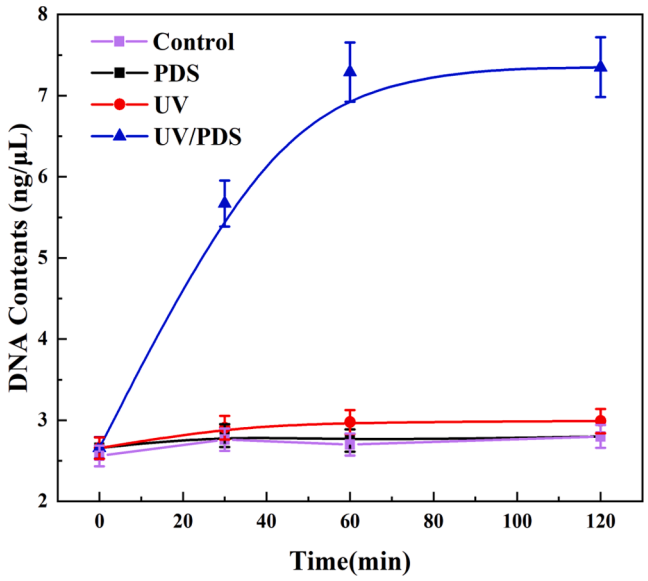

Fig. 5. The change of extracellular DNA concentration in *U. marinum* under different conditions. (*U. marinum* = 1 × 10^8 cells·mL^{-1}, PDS = 1 mM, Light power = 14 W, T = 298.15 K, pH = 8).

while CAT can further promote the conversion of H_2O_2 to H_2O and O_2 [64]. Thus, a higher SOD and CAT activity suggests the cells are experiencing a more serious oxidative stress attack from the environment. The activities of the important intracellular antioxidant enzymes including CAT and SOD of *U. marinum* were monitored respectively during the inactivation process [65]. As shown in Fig. 6(A), neither CAT nor SOD showed obvious changes in the single PDS system. The change trend of CAT and SOD was the same in the single UV irradiation and UV/PDS system, both rising first and then falling. In the initial 120 s, the rapid increase of the activities indicating that the *U. marinum* cells were encountering severe oxidative stress from the environment. The increases of the activities were greater in the UV/PDS system than that under the single UV irradiation indicating that there was a large amount of oxidative radicals such as $\bullet SO_4^-$ and •OH attacking the *U. marinum* cells. The result was consistent with the detection and contribution analysis of radicals. After 120 s, both CAT and SOD activities gradually decreased as the inactivation process progressed. The phenomenon may be explained by that a large number of oxidative species produced in the system had exceeded the load of *U. marinum* stress system and destroyed its defense function [38].

Transcriptomics, proteomics and metabolomics can reveal the change of genes transcription, protein expression and the metabolism of organisms, respectively [66]. For the research on the biological inactivation mechanism by AOT, only a few relevant literatures based on •OH

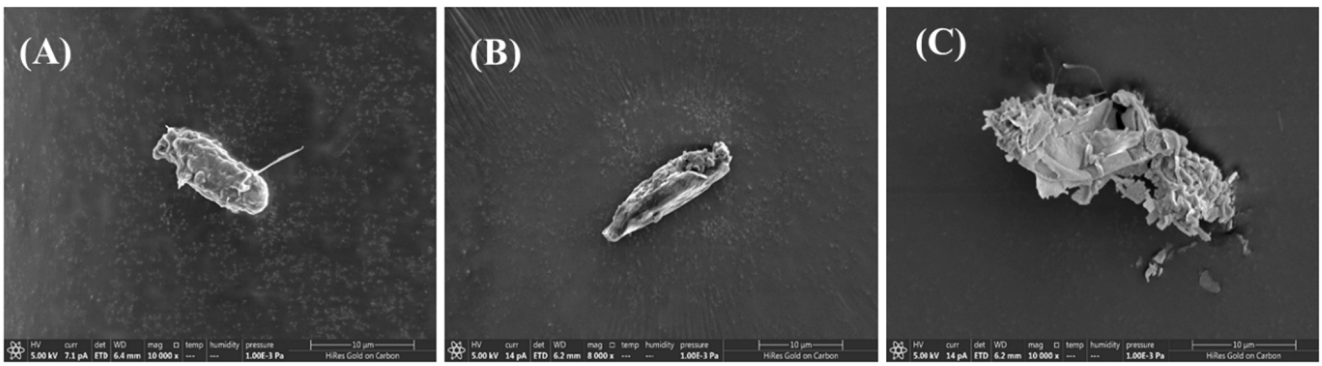

Fig. 4. SEM images of *U. marinum* cells under different systems. **(A)** Control; **(B)** UV irradiation; **(C)** UV/PDS. (*U. marinum* = 1 × 10^8 cells·mL^{-1}, PDS = 1 mM, Light power = 14 W, T = 298.15 K, pH = 8).

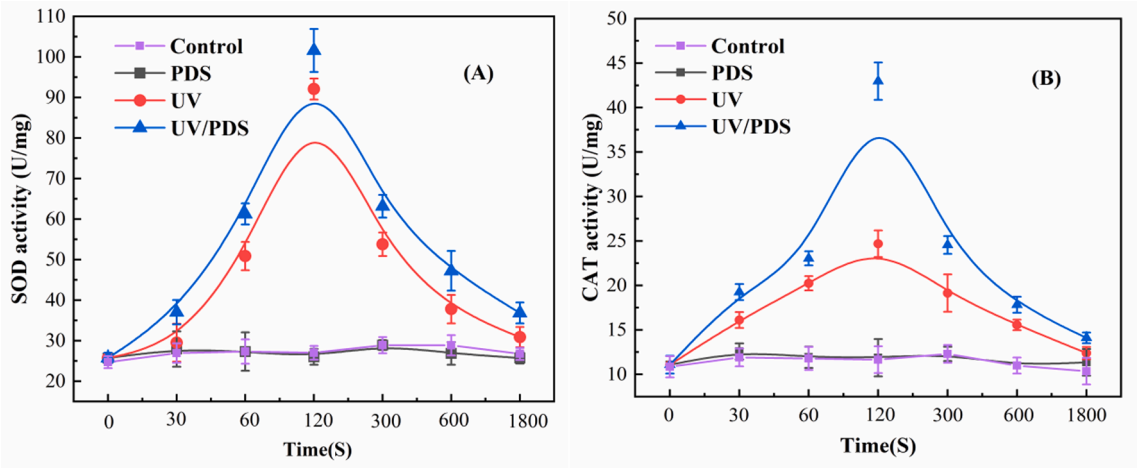

Fig. 6. SOD and CAT activity of *U. marinum*. **(A)** SOD activity; **(B)** CAT activity (*U. marinum* = 1×10^8 cells·mL^{-1}, PDS = 1 mM, Light power = 14 W, T = 298.15 K, pH = 8).

were analyzed by omics. For example, Li et al. described the photocatalytic inactivation mechanism of *E. coli*. Through transcriptomic analysis, it was found that •OH inhibited genes that resist cell membrane damage and oxidative stress response [67]. Therefore, besides the cell integrity and the antioxidant enzyme activity, the inactivation mechanism was analyzed by the omics through the overall response of *U. marinum* after treated with UV / PDS. The details of omics analysis were described in SI Text S9. The quality and feasibility of omics analysis,

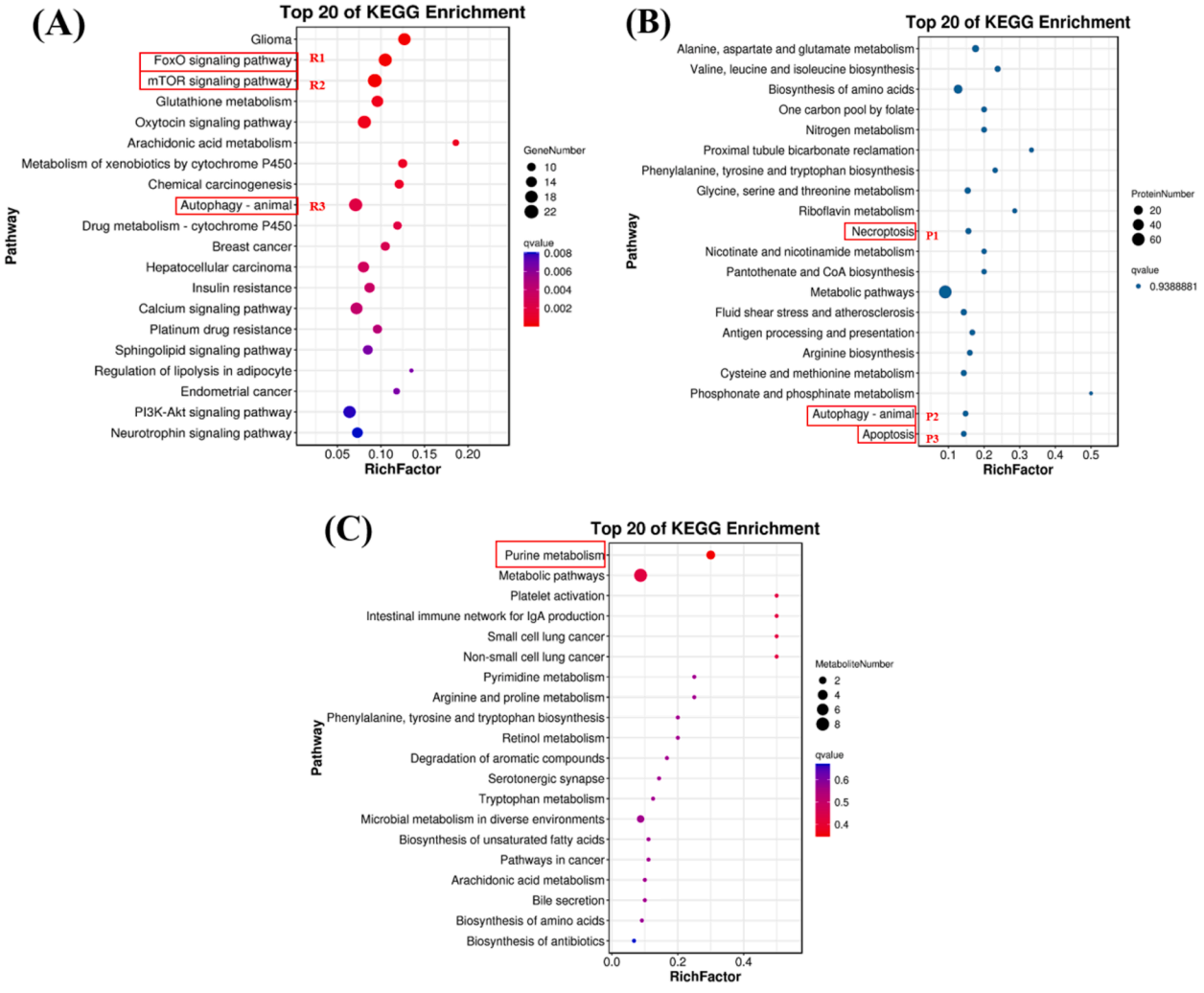

Fig. 7. KEGG pathway enrichment analysis of *U. marinum*. **(A)** Transcriptomics; **(B)** Proteomics; **(C)** Metabolomics. (*U. marinum* = 1×10^8 cells·mL^{-1}, PDS = 1 mM, Light power = 14 W, T = 298.15 K, pH = 8).

were shown in Fig. S7A-S9A. Differential expression of genes, proteins and metabolites were visualized in the heatmap and volcano plot (shown in SI Fig. S7B, C—S9B, C). To evaluate the potential function of differentially expressed genes (DEGs), differentially expressed proteins (DEPs) and differential metabolites (DEMs), pathway enrichment analysis based on the KEGG database was performed. As shown in Fig. 7(A), the signal pathways related to the oxidative stress and apoptotic function appeared in transcriptomics (R1-*R*3) and proteomics (*P*1-*P*3). Multiple DEGs (MKK3、YPK1、pkaC、gad8、Pdpk1, etc.) appeared in the transcriptome $F_{OX}O$ signaling pathway. For example, MKK3 was a double threonine / tyrosine protein kinase, which could resist apoptosis through specific phosphorylation and activation of p38 mitogen activated protein kinase [68]. Apoptosis was the independent and orderly death of cells controlled by genes to maintain the stability of internal environment [69]. Therefore, the decrease of MKK3 expression may be one of the reasons for *U.marinum* cell inactivation. As shown in Fig. 7(B), there are also many DEPs (SEN102、cpz-1、PRDX2、ACT1A, etc.) in proteome apoptosis pathway. For example, PRDX2 plays an important role in cell oxidative defense [70]. Oxidative stress will lead to cell apoptosis and the decrease of its expression may be another reason for *U. marinum* cell inactivation. As shown in Fig. 7(C), metabonomic analysis showed that the DEMs were significantly enriched in the purine metabolism pathway, in which the expression of differential metabolites including hypoxanthin, guanosine and uric acid decreased resulting in abnormal nucleotide composition in cells. There were also adverse effects on cell growth and metabolism resulting in *U.marinum* cell inactivation. The above results showed that the free radicals generated in the UV/PDS system affected the genes, proteins expression and metabolites of *U.marinum* and caused the inactivation.

3.5. Disinfection by-products formation during UV/PDS treatment of marine water

Reactive radicals could be produced during the UV/PDS treatment in the existence of a high concentration of halogen ions, which were able to attack some contaminants and bond to them or the formed intermediates, thereby resulting in the generation of disinfection by-products and the increase in the ClO_3^-, BrO_3^- and halogenated byproducts concentration. AOX is a parameter determining the overall quantity of organically bonded halogens in an environment. The

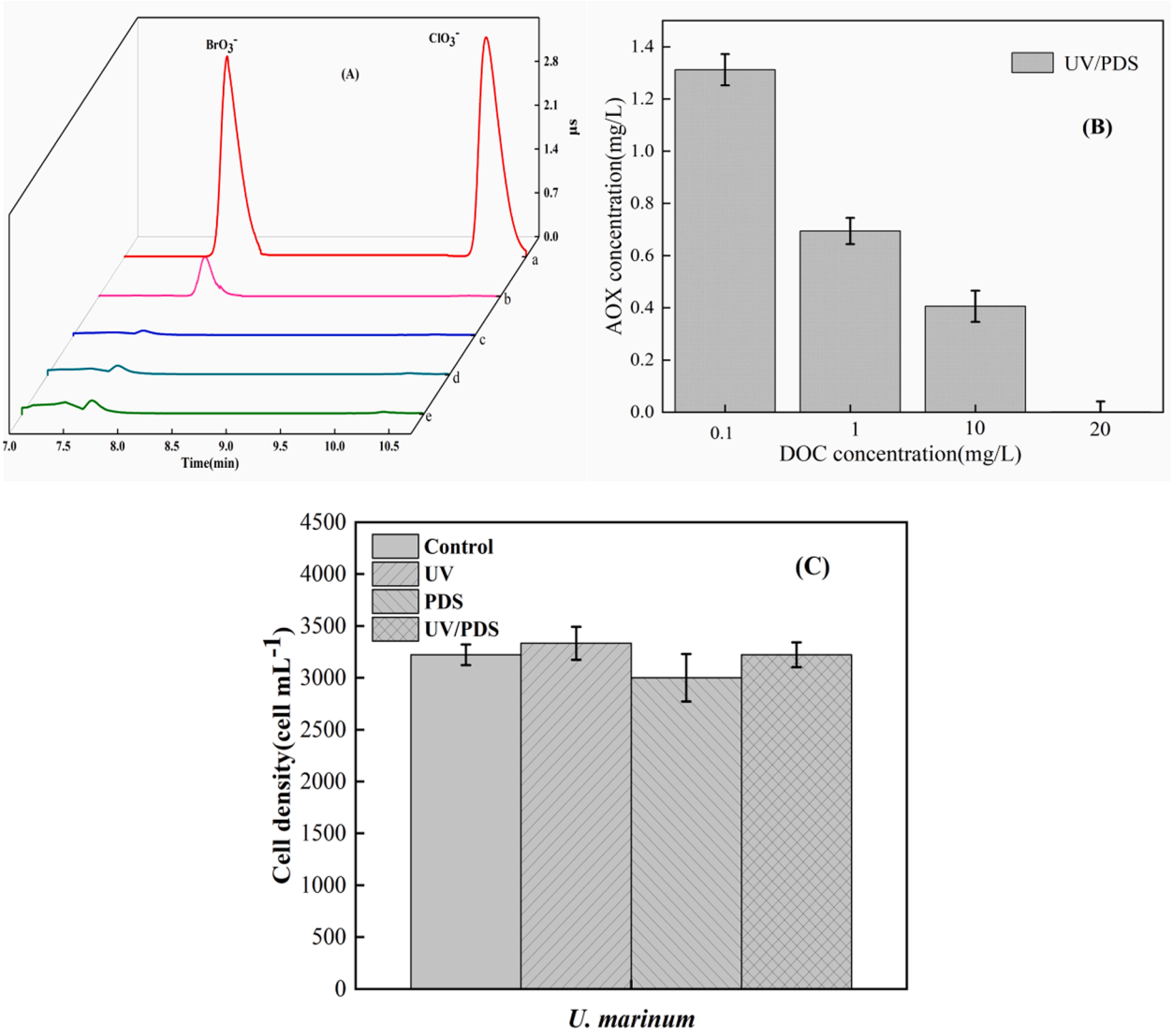

Fig. 8. Biotoxicity analysis of the UV/PDS system. **(A)** The concentration of ClO_3^- and BrO_3^- in marine water at different concentrations of HA. a: reference materials, b: 0.01 mM HA, c: 0.1 mM HA, d: 1 mM HA, e: actual seawater. **(B)** The concentration of AOX in marine water at different concentrations of HA. **(C)** Growth inhibition of *U. marinum* from water samples treated with different systems. (*U. marinum* = 1×10^3 cells·mL^{-1}, PDS = 1 mM, Light power = 14 W, T = 298.15 K, pH = 8).

generation of halogenated byproducts can be quantified directly by detecting the concentration of AOX.

The concentrations of ClO_3^-, BrO_3^- and AOX produced by the UV/PDS reaction were studied in marine water with different amounts of HA and actual marine water. The qualitative analysis of ClO_3^- and BrO_3^- in various marine water bodies was carried out. As shown in Fig. 8(A), ClO_3^- and BrO_3^- were not detected when the HA concentration was 0.01 mM, 0.1 mM and 1 mM, but the characteristic peak of BrO_3^- was displayed when the HA concentration was as low as 0.01 mM. As shown in Fig. 8(B), when the concentration of HA was 0.01 mM, 0.1 mM and 1 mM, the concentration of AOX is 1.3119 mg·L^{-1}, 0.6939 mg·L^{-1} and 0.4059 mg·L^{-1} respectively. The concentration of AOX measured in the actual sea water was 0.011 mg·L^{-1}. With the increase of HA concentration, the content of AOX is reduced. In order to verify the effect of the DBPs in the UV/PDS system to the growth of organisms, toxicological experiments were conducted. As shown in Fig. 8(C), the reaction seawater did not obviously inhibit the growth of *U. marinum*, which indicated that the UV/PDS systems was environmentally friendly.

The results showed that organic matter would inhibit ClO_3^-, BrO_3^- and AOX, the higher the concentration of organic matter, the lower the concentration of the DBPs. The reason should be attributed to that the reaction of HA with radicals, which reduces the amount of effective $\bullet SO_4^-$ in the UV/PDS system and reduces the reaction with halogen ions. As reported by Fang et al., during the degradation of micro pollutant, the percentages of conversion from Br^- to BrO_3^- were significant if water contained lower quantities of natural organic matter in UV/PDS system [71]. In addition, Xie et al. reported that a considerable increase in the AOX concentration was discovered in both UV/PDS under the condition that total organic carbon concentration was minimized [72].

In marine aquaculture water, the concentration of DOC was usually greater than 20 mg·L^{-1}, so there was no generation potential of the DBPs. However, the IMO management of ballast water stipulates that ballast water must be exchanged on the high seas in order to control the biological invasion caused. Due to the difference of organic matter content in various sea areas, when the organic matter content is lower than 1 mg·L^{-1}, UV/PDS disinfection system may produce DBPs. Therefore, it is recommended to add some ship domestic sewage as carbon source to avoid the generation of DBPs and the domestic sewage can also be treated simultaneously.

3.6. Economic analysis of UV/PDS

To explore the potential application of UV/PDS for *U. Marinum* inactivation, the cost of the process was calculated preliminarily. According to International Union of Pure and Applied Chemistry (IUPAC) guidelines, electrical energy per order (EE/O) can be defined as the electrical energy dose necessary to reduce the concentration of a pollutant by one order of magnitude. For pollutant concentration lower than 100 mg/L, the value of EE/O in UV-based AOTs and the total cost can be calculated by Eq. (15) and Eq. (16), respectively [73].

$$EE/O = \frac{PT}{60 \times V \times log(N_0/N_t)} \quad (15)$$

$$C_T = 1.45 \times EE/O \times C_E + C_0 \quad (16)$$

P = the light power (W);
t = the treatment time (min);
V = the total treated bulk (L);
N_0 = the original concentrations of ciliate *U. marinum* (cells mL^{-1});
N_t = the final concentrations of ciliate *U. marinum* (cells mL^{-1});
C_T = the total system cost ($ m^{-3});
C_E = the electricity bills ($ KWh^{-1});
C_0 = the cost of oxidant ($ g^{-1}).

The electricity cost is 0.08 $ KWh^{-1} (45 % of total electricity cost as maintenance cost) and PDS cost is 0.006 $ g^{-1} [74]. As can be seen from Table 1, the total cost of UV/PDS for inactivation of *U. marinum* was calculated to be 0.062 $ m^{-3}. As reported, the pureballast water treatment system was approved by the IMO and the cost of ballast water treatment was approximately 0.07 $ m^{-3} [75]. The cost of UV/PDS is similar to that of the pureballast water treatment system indicating that UV/PDS is economically reasonable. However, accurate economic costs still need to be evaluated after pilot test and larger scale expansion.

Table 1
The costs of the UV/PDS oxidation systems.

EE/O (kWh m^{-3} $order^{-1}$)	Electricity bills ($ KWh^{-1})	Oxidant cost ($ g^{-1})	Total ($ m^{-3})
0.53	0.08	0.00014	0.062

4. Conclusions

•OH based AOT can inactivate microorganisms efficiently while avoiding the generation of organic DBPs. AOTs have received extensive attentions in disinfection of various water bodies. The redox potential of $\bullet SO_4^-$ is similar to that of •OH, but the half-life is longer. Many researchers have reported that $\bullet SO_4^-$ based advanced oxidation technologies (ASOT) was very effective in inactivating bacteria and algae in marine water. But so far ASOT has not been used to inactivate protozoa. This study investigated the inactivation effect on special protozoa ciliate *U. marinum*, a common unicellular organism which lived freely in marine water such as the ballast water as well as the marine aquaculture water. It was elucidated that the UV/PDS system was very effective for *U. marinum* inactivation. Moreover, this study is among the first to investigate the biological inactivation mechanism by omics including transcriptomics, proteomics and metabolomics. The results showed that except the damage of cell integrity and enzyme activity, the free radicals generated in the UV/PDS system affected the genes, proteins expression and metabolites of *U.marinum*. Because the organic matter would inhibit ClO_3^-, BrO_3^- and AOX adding carbon source may be one of the solutions to control the inorganic DBPs. It provides theoretical support for the development of green and efficient marine water disinfection technology.

CRediT authorship contribution statement

Yuanyuan Zhang: Investigation, Writing – original draft, Writing – review & editing, Funding acquisition. **Kunling Huang:** Writing – original draft. **Xuan Chen:** Methodology. **Min Wei:** Methodology. **Xiaopeng Yu:** Methodology. **Hongfei Su:** Methodology. **Pin Gan:** Methodology. **Kefu Yu:** Conceptualization, Writing – review & editing, Validation, Funding acquisition.

Declaration of Competing Interest

The authors declare that they have no known competing financial interests or personal relationships that could have appeared to influence the work reported in this paper.

Data availability

Data will be made available on request.

Acknowledgements

This study was supported by the Natural Science Foundation of Guangxi Province (2020GXNSFAA159135), the National Science Foundation China (No.42030502, No.42090041), the College Students' Innovative Entrepreneurial Training Plan Program (202010593245, 202110593171).

Appendix A. Supplementary material

Supplementary data to this article can be found online at https://doi.org/10.1016/j.seppur.2022.122563.

References

[1] A.T. Rachmadi, M. Kitajima, T. Kato, H. Kato, S. Okabe, D. Sano, Required chlorination doses to fulfill the credit value for disinfection of enteric viruses in water: a critical review, Environ. Sci. Technol. 54 (4) (2020) 2068–2077.

[2] L. Chen, Y. Deng, S.K. Dong, H. Wang, P. Li, H.Y. Zhang, W.H. Chu, The occurrence and control of waterborne viruses in drinking water treatment: a review, Chemosphere 281 (2021), 130728, https://doi.org/10.1016/j.chemosphere.2021.130728.

[3] J. Wang, J. Shen, D. Ye, X. Yan, Y.J. Zhang, W.J. Yang, X.W. Li, J.Q. Wang, L. B. Zhang, L.J. Pan, Disinfection technology of hospital wastes and wastewater: suggestions for disinfection strategy during coronavirus Disease 2019 (COVID-19) pandemic in China, Environ. Pollut. 262 (2020), 114665, https://doi.org/10.1016/j.envpol.2020.114665.

[4] S. Hand, R.D. Cusick, Electrochemical disinfection in water and wastewater treatment: identifying impacts of water quality and operating conditions on performance, Environ. Sci. Technol. 55 (2021) 3470–3482, https://doi.org/10.1021/acs.est.0c06254.

[5] W.J. Wang, P. Liao, G.Y. Li, H. Chen, J.Y. Cen, S.H. Lu, P.K. Wong, T.C. An, Photocatalytic inactivation and destruction of harmful microalgae Karenia mikimotoi under visible-light irradiation: insights into physiological response and toxicity assessment, Environ. Res. 198 (2021), 111295, https://doi.org/10.1016/j.envres.2021.111295.

[6] X.X. Wang, Y.L. Huang, K. Zhang, Y. Shi, Z. Lu, Y.H. Wang, Inactivation effect and mechanisms of combined ultraviolet and metal-doped nano-$TiO_{(2)}$ on treating *Escherichia coli* and *Enterococciin* ballast water, Environ. Sci. Pollut. Res. 27 (2020) 40286–40295, https://doi.org/10.1007/s11356-020-10034-5.

[7] Y. Kim, S.D. Snow, V. Reichel-Deland, M. Maghsoodi, G.M. Langlois, V.V. Tarabara, J.B. Rose, Current status and recommendations toward a virus standard for ballast water, Manage. Biol. Invasions 10 (2019) 267–284, https://doi.org/10.3391/mbi.2019.10.2.04.

[8] G. Du, L. Qu, K. Shang, C. Sun, C. Wang, P. Gao, Ciliate *Uronema marinum* is the causative agent of scuticociliatosis in farm raised turbot *Scophthalmus maximus*, J. Oceanol. Limnol. 37 (2019) 1726–1735, https://doi.org/10.1007/s00343-020-8305-8.

[9] E. Geba, D. Aubert, L. Durand, S. Escotte, S. La Carbona, C. Cazeaux, I. Bonnard, F. Bastien, M.P. Ladeiro, J.P. Dubey, I. Villena, A. Geffard, A. Bigot-Clivot, Use of the bivalve *Dreissena polymorpha* as a biomonitoring tool to reflect the protozoan load in freshwater bodies, Water Res. 170 (2020), 115297, https://doi.org/10.1016/j.watres.2019.115297.

[10] IMO. International Convention for the Control and Management of Ships' Ballast Water and Sediments. **2004**.

[11] V.K. Sharma, N. Johnson, L. Cizmas, T.J. McDonald, H. Kim, A review of the influence of treatment strategies on antibiotic resistant bacteria and antibiotic resistance genes, Chemosphere 150 (2016) 702–714, https://doi.org/10.1016/j.chemosphere.2015.12.084.

[12] T. Azuma, T. Hayashi, On-site chlorination responsible for effective disinfection of wastewater from hospital, Sci. Total Environ. 776 (2021), 145951, https://doi.org/10.1016/j.scitotenv.2021.145951.

[13] Y.W. Cai, T. Sun, G.Y. Li, T.C. An, Traditional and emerging water disinfection technologies challenging the control of antibiotic-resistant bacteria and antibiotic resistance genes, ACS ES&T Eng 1 (2021) 1046–1064, https://doi.org/10.1021/acsestengg.1c00110.

[14] Y.Y. Zhang, C. Rong, Y.Q. Song, Y.H. Wang, J.Y. Pei, X.Y. Tang, R.J. Zhang, K. F. Yu, Oxidation of the antibacterial agent norfloxacin during sodium hypochlorite disinfection of marine culture water, Chemosphere 182 (2017) 245–254, https://doi.org/10.1016/j.chemosphere.2017.05.023.

[15] Y.Y. Zhang, Z.H. Pan, C. Rong, Y.A. Shao, Y.H. Wang, K.F. Yu, Transformation of antibacterial agent roxithromycin in sodium hypochlorite disinfection process of different water matrices, Sep. Purif. Technol. 212 (2019) 528–535, https://doi.org/10.1016/j.seppur.2018.11.061.

[16] A.-A. Simpson, W.A. Mitch, Chlorine and ozone disinfection and disinfection byproducts in postharvest food processing facilities: a review, Crit. Rev. Env. Sci. Technol. 52 (11) (2022) 1825–1867.

[17] G. Wen, X.Q. Xu, H. Zhu, T.L. Huang, J. Ma, Inactivation of four genera of dominant fungal spores in groundwater using UV and UV/PMS: efficiency and mechanisms, Chem. Eng. J. 328 (2017) 619–628, https://doi.org/10.1016/j.cej.2017.07.055.

[18] J.X. Yang, Z.J. Dong, C.C. Jiang, C. Wang, H. Liu, An overview of bromate formation in chemical oxidation processes: occurrence, mechanism, influencing factors, risk assessment, and control strategies, Chemosphere 237 (2019), 124521, https://doi.org/10.1016/j.chemosphere.2019.124521.

[19] Z. Liu, G. Wen, Y.L. Ni, S.B. Wang, S. Wang, Y. Yu, T.L. Huang, J. Ma, Inhibition of bromate formation in the ozone/peroxymonosulfate process by ammonia, ammonia-chlorine and chlorine-ammonia pretreatment: comparisons with ozone alone, Sep. Purif. Technol. 278 (2022), 119600, https://doi.org/10.1016/j.seppur.2021.119600.

[20] Y.D. Chen, X.G. Duan, X. Zhou, R.P. Wang, S.B. Wang, N.Q. Ren, S.H. Ho, Advanced oxidation processes for water disinfection: features, mechanisms and prospects, Chem. Eng. J. 409 (2021), 128207, https://doi.org/10.1016/j.cej.2020.128207.

[21] J.R. Bu, X.K. Zhou, H. Liu, C.M. Lin, Supercritical fenton oxidation: new advanced oxidation technology, J. Environ. Eng. 146 (2020) 1943–7870, https://doi.org/10.1061/(asce)ee.1943-7870.0001660.

[22] S. Ma, K. Kim, S. Chun, S.Y. Moon, Y. Hong, Plasma-assisted advanced oxidation process by a multi-hole dielectric barrier discharge in water and its application to wastewater treatment, Chemosphere 243 (2020), 125377, https://doi.org/10.1016/j.chemosphere.2019.125377.

[23] W. Chu, Y.R. Wang, H.F. Leung, Synergy of sulfate and hydroxyl radicals in UV/$S_2O_8^{2-}$/H_2O_2 oxidation of iodinated X-ray contrast medium iopromide, Chem. Eng. J. 178 (2011) 154–160, https://doi.org/10.1016/j.cej.2011.10.033.

[24] S. Giannakis, K.Y.A. Lin, F. Ghanbari, A review of the recent advances on the treatment of industrial wastewaters by sulfate radical-based advanced oxidation processes (SR-AOPs), Chem. Eng. J. 406 (2021), 127083, https://doi.org/10.1016/j.cej.2020.127083.

[25] H.W. Luo, Y.F. Zeng, Y. Cheng, D.Q. He, X.L. Pan, Activation of peroxymonosulfate by iron oxychloride with hydroxylamine for ciprofloxacin degradation and bacterial disinfection, Sci. Total Environ. 799 (2021), 149506, https://doi.org/10.1016/j.scitotenv.2021.149506.

[26] R.Y. Xiao, K. Liu, L. Bai, D. Minakata, Y. Seo, R.K. Goktas, D.D. Dionysiou, C. J. Tang, Z.S. Wei, R. Spinney, Inactivation of pathogenic microorganisms by sulfate radical: present and future, Chem. Eng. J. 371 (2019) 222–232, https://doi.org/10.1016/j.cej.2019.03.296.

[27] X.X. Pan, J. Chen, N.N. Wu, Y.M. Qi, X.X. Xu, J.L. Ge, X.H. Wang, C.G. Li, R.J. Qu, V.K. Sharma, Z.Y. Wang, Degradation of aqueous 2,4,4'-Trihydroxybenzophenone by persulfate activated with nitrogen doped carbonaceous materials and the formation of dimer products, Water Res. 143 (2018) 176–187, https://doi.org/10.1016/j.watres.2018.06.038.

[28] X.L. Zhang, M.B. Feng, L.S. Wang, R.J. Qu, Z.Y. Wang, Catalytic degradation of 2-phenylbenzimidazole-5-sulfonic acid by peroxymonosulfate activated with nitrogen and sulfur co-doped CNTs-COOH loaded $CuFe_2O_4$, Chem. Eng. J. 307 (2017) 95–104, https://doi.org/10.1016/j.cej.2016.08.078.

[29] H. Liu, P. Sun, M.B. Feng, H.X. Liu, S.G. Yang, L.S. Wang, Z.Y. Wang, Nitrogen and sulfur co-doped CNT-COOH as an efficient metal-free catalyst for the degradation of UV filter BP-4 based on sulfate radicals, Appl. Catal. B Environ 187 (2016) 1–10, https://doi.org/10.1016/j.apcatb.2016.01.036.

[30] I. Michael-Kordatou, M. Iacovou, Z. Frontistis, E. Hapeshi, D.D. Dionysiou, D. Fatta-Kassinos, Erythromycin oxidation and ERY-resistant Escherichia coli inactivation in urban wastewater by sulfate radical-based oxidation process under UV-C irradiation, Water Res. 85 (2015) 346–358, https://doi.org/10.1016/j.watres.2015.08.050.

[31] P.Z. Sun, C. Tyree, C.H. Huang, Inactivation of *Escherichia coli*, *Bacteriophage MS2*, and *Bacillus Spores* under UV/H_2O_2 and UV/peroxydisulfate advanced disinfection conditions, Environ. Sci. Technol. 50 (2016) 4448–4458, https://doi.org/10.1021/acs.est.5b06097.

[32] C.Y. Chen, Z.H. Wu, S.D. Hou, A.N. Wang, J.Y. Fang, Transformation of gemfibrozil by the interaction of chloride with sulfate radicals: radical chemistry, transient intermediates and pathways, Water Res. 209 (2022), 117944, https://doi.org/10.1016/j.watres.2021.117944.

[33] R.E. Huie, C.L. Clifton, Temperature dependence of the rate constants for reactions of the sulfate radical, $SO_4^{\cdot}$, with anions, J. Phys. Chem. 94 (1990) 8561–8567, https://doi.org/10.1021/j100386a015.

[34] L.P. Wang, C.S. Ye, L.Z. Guo, C.Y. Chen, X.J. Kong, Y.Q. Chen, L.F. Shu, P. Wang, X. Yu, J.Y. Fang, Assessment of the UV/chlorine process in the disinfection of pseudomonas aeruginosa: efficiency and mechanism, Environ. Sci. Technol. 55 (2021) 9221–9230, https://doi.org/10.1021/acs.est.1c00645.

[35] M. Bai, Z. Zhang, X. Xue, X. Yang, L. Hua, D. Fan, Killing effects of hydroxyl radical on algae and bacteria in ship's ballast water and on their cell morphology, Plasma Chem. Plasma Process. 30 (6) (2010) 831–840.

[36] J. Moreno-Andres, N. Ambauen, O. Vadstein, C. Halle, A. Acevedo-Merino, E. Nebot, T. Meyn, Inactivation of marine heterotrophic bacteria in ballast water by an electrochemical advanced oxidation process, Water Res. 140 (2018) 377–386, https://doi.org/10.1016/j.watres.2018.04.061.

[37] W. Wang, H. Wang, G. Li, T. An, H. Zhao, P.K. Wong, Catalyst-free activation of persulfate by visible light for water disinfection: Efficiency and mechanisms, Water Res. 157 (2019) 106–118, https://doi.org/10.1016/j.watres.2019.03.071.

[38] J.G. Muller, P. Zheng, S.E. Rokita, C.J. Burrows, DNA and RNA modification promoted by $[Co(H_2O)_6]Cl_2$ and $KHSO_5$: guanine selectivity, temperature dependence, and mechanism, J. Am. Chem. Soc. 118 (1996) 2320–2325, https://doi.org/10.1021/ja952518m.

[39] R.Y. Xiao, L. Bai, K. Liu, Y. Shi, D. Minakata, C.H. Huang, R. Spinney, R. Seth, D. D. Dionysiou, Z.S. Wei, P.Z. Sun, Elucidating sulfate radical-mediated disinfection profiles and mechanisms of *Escherichia coli* and *Enterococcus faecalis* in municipal wastewater, Water Res. 173 (2020), 115552, https://doi.org/10.1016/j.watres.2020.115552.

[40] H. Liu, Z.G. Wang, W.H. Xu, J. Zeng, L.X. Li, S.L. Li, Z. Gao, Bacillus pumilus LZP02 promotes rice root growth by improving carbohydrate metabolism and phenylpropanoid biosynthesis, Mol. Plant Microbe Interact. 33 (2020) 1222–1231, https://doi.org/10.1094/mpmi-04-20-0106-r.

[41] Y.T. Huang, K. Zhang, M.M. Jiang, J.Y. Ni, J.R. Chen, L. Li, J. Deng, Y. Zhu, J. Y. Mao, X.M. Gao, G.W. Fan, Regulation of energy metabolism by combination therapy attenuates cardiac metabolic remodeling in heart failure, Int. J. Biol. Sci. 16 (2020) 3133–3148, https://doi.org/10.7150/ijbs.49520.

[42] J.S. Ramsey, E.L. Chin, J.D. Chavez, S. Saha, D. Mischuk, J. Mahoney, J. Mohr, F. M. Robison, E. Mitrovic, Y.M. Xu, S.R. Strickler, N. Fernandez, X.F. Zhong,

M. Polek, K.E. Godfrey, J.J. Giovannoni, L.A. Mueller, C.M. Slupsky, J.E. Bruce, M. Heck, Longitudinal transcriptomic, proteomic, and metabolomic analysis of citrus limon response to graft inoculation by candidatus Liberibacter asiaticus, J. Proteome Res. 19 (2020) 2247–2263, https://doi.org/10.1021/acs.jproteome.9b00802.

[43] H. Zeng, L. Shen, N. Lin, Z. Zhan, Effect of different culture conditions on the population growth of *Uronema marinum*, J. Fujian Norm. Univ. (Nat. Sci. Ed.) 31 (2015) 87–92.

[44] R.C. Zhang, P.Z. Sun, T.H. Boyer, L. Zhao, C.H. Huang, Degradation of pharmaceuticals and metabolite in synthetic human urine by UV, UV/H_2O_2, and UV/PDS, Environ. Sci. Technol. 49 (2015) 3056–3066, https://doi.org/10.1021/es504799n.

[45] J. Zhao, J.D. Peng, R. Yin, M.G. Fan, X. Yang, C. Shang, Multi-angle comparison of UV/chlorine, UV/monochloramine, and UV/chlorine dioxide processes for water treatment and reuse, Water Res. 217 (2022), 118414, https://doi.org/10.1016/j.watres.2022.118414.

[46] Q. Wang, Y. Zhang, A. Guo, C. Xiong, The effects of watermelon rind on population growth of paramoecium caudatum, J. Yunnan Agric. Univ 31 (2016) 1140–1144.

[47] H.Z. Liu, T.A. Bruton, F.M. Doyle, D.L. Sedlak, In situ chemical oxidation of contaminated groundwater by persulfate: decomposition by Fe(III) and Mn(IV) containing oxides and aquifer materials, Environ. Sci. Technol. 48 (2014) 10330–10336, https://doi.org/10.1021/es502056d.

[48] M.B. Feng, R.J. Qu, X.L. Zhang, P. Sun, Y.X. Sui, L.S. Wang, Z.Y. Wang, Degradation of flumequine in aqueous solution by persulfate activated with common methods and polyhydroquinone-coated magnetite/multi-walled carbon nanotubes catalysts, Water Res. 85 (2015) 1–10, https://doi.org/10.1016/j.watres.2015.08.011.

[49] Y. Zhang, M. Wei, K. Huang, K. Yu, J. Liang, F. Wei, J. Huang, X. Yin, Inactivation of *E. coli* and *Streptococcus agalactiae* by UV/persulfate during marine aquaculture disinfection, Environ. Sci. Pollut. Res. 29 (30) (2022) 45421–45434.

[50] Y.Y. Zhang, L.Y. Li, Z.H. Pan, Y.J. Zhu, Y.N. Shao, Y.H. Wang, K.F. Yu, Degradation of sulfamethoxazole by UV/persulfate in different water samples: influential factors, transformation products and toxicity, Chem. Eng. J. 379 (2020), 122354, https://doi.org/10.1016/j.cej.2019.122354.

[51] K. Oguma, Inactivation of feline calicivirus using ultraviolet light-emitting diodes, FEMS Microbiol. Lett. 365 (2018), fny194, https://doi.org/10.1093/femsle/fny194.

[52] S. Li, Y. Tao, X.M. Zhan, G.H. Dao, H.Y. Hu, UV-C irradiation for harmful algal blooms control: a literature review on effectiveness, mechanisms, influencing factors and facilities, Sci. Total Environ. 723 (2020), 137986, https://doi.org/10.1016/j.scitotenv.2020.137986.

[53] M. Raeiszadeh, F. Taghipour, Inactivation of microorganisms by newly emerged microplasma UV lamps, Chem. Eng. J. 413 (2021), 127490, https://doi.org/10.1016/j.cej.2020.127490.

[54] X.J. Hou, G.M. Zhan, X.P. Huang, N. Wang, Z.H. Ai, L.Z. Zhang, Persulfate activation induced by ascorbic acid for efficient organic pollutants oxidation, Chem. Eng. J. 382 (2020), 122355, https://doi.org/10.1016/j.cej.2019.122355.

[55] M. Alhamd, T. Tabatabaie, I. Parseh, F. Amiri, N. Mengelizadeh, Magnetic $CuNiFe_2O_4$ nanoparticles loaded on multi-walled carbon nanotubes as a novel catalyst for peroxymonosulfate activation and degradation of reactive black 5, Environ. Sci. Pollut. R 28 (2021) 57099–57114, https://doi.org/10.1007/s11356-021-14590-2.

[56] R.S. Magazinovic, B.C. Nicholson, D.E. Mulcahy, D.E. Davey, Bromide levels in natural waters: its relationship to levels of both chloride and total dissolved solids and the implications for water treatment, Chemosphere 57 (2004) 329–335, https://doi.org/10.1016/j.chemosphere.2004.04.056.

[57] X.Y. Yu, Z.C. Bao, J.R. Barker, Free radical reactions involving $Cl^{\bullet}$, $Cl2^{-\bullet}$, and $SO_4^{\bullet}$ in the 248 nm photolysis of aqueous solutions containing $S_2O_8^{2-}$ and Cl^-, J. Phys. Chem. A 108 (2004) 295–308, https://doi.org/10.1021/jp036211i.

[58] D. Libera, H. Elie, Flash photolysis of peroxydisulfate ions in aqueous solutions. The sulfate and ozonide radical anions, J. Phys. Chem. 1967.

[59] G.V. Buxton, C.L. Greenstock, W.P. Helman, A.B. Ross, Critical Review of rate constants for reactions of hydrated electrons, hydrogen atoms and hydroxyl radicals (·OH/·O^-) in Aqueous Solution, J. Phys. Chem. Ref. Data 17 (2) (1988) 513–886.

[60] C.D. Qi, X.T. Liu, C.Y. Lin, X.H. Zhang, J. Ma, H.B. Tan, W. Ye, Degradation of sulfamethoxazole by microwave-activated persulfate: Kinetics, mechanism and acute toxicity, Chem. Eng. J. 249 (2014) 6–14, https://doi.org/10.1016/j.cej.2014.03.086.

[61] J. Saien, M. Osali, A.R. Soleymani, UV/persulfate and UV/hydrogen peroxide processes for the treatment of salicylic acid: effect of operating parameters, kinetic, and energy consumption, Desalin, Water Treat 56 (2015) 3087–3095, https://doi.org/10.1080/19443994.2014.963156.

[62] S. Sontakke, J. Modak, G. Madras, Photocatalytic inactivation of *Escherischia coli* and *Pichia pastoris* with combustion synthesized titanium dioxide, Chem. Eng. J. 165 (2010) 225–233, https://doi.org/10.1016/j.cej.2010.09.021.

[63] F.Z. Zeng, S. Cao, W.B. Jin, X. Zhou, W.Q. Ding, R.J. Tu, S.F. Han, C.P. Wang, Q. J. Jiang, H. Huang, F. Ding, Inactivation of chlorine-resistant bacterial spores in drinking water using UV irradiation, UV/Hydrogen peroxide and UV/Peroxymonosulfate: Efficiency and mechanism, J. Clean Prod. 243 (2020), 118666, https://doi.org/10.1016/j.jclepro.2019.118666.

[64] W.J. Wang, T.W. Ng, W.K. Ho, J.H. Huang, S.J. Liang, T.C. An, G.Y. Li, J.C. Yu, P. K. Wong, $CdIn_2S_4$ microsphere as an efficient visible-light-driven photocatalyst for bacterial inactivation: synthesis, characterizations and photocatalytic inactivation mechanisms, Appl. Catal. B 129 (2013) 482–490, https://doi.org/10.1016/j.apcatb.2012.09.054.

[65] H.B. Xu, Y.P. Zhu, M.R. Du, Y.Q. Wang, S.Y. Ju, R.N. Ma, Z. Jiao, Subcellular mechanism of microbial inactivation during water disinfection by cold atmospheric-pressure plasma, Water Res. 188 (2021), 116513, https://doi.org/10.1016/j.watres.2020.116513.

[66] A. Mishra, K. Medhi, P. Malaviya, I.S. Thakur, Omics approaches for microalgal applications: prospects and challenges, Bioresour. Technol. 291 (2019), 121890, https://doi.org/10.1016/j.biortech.2019.121890.

[67] Y. Li, J. Zhao, G.S. Zhang, L.L. Zhang, S.Y. Ding, E.X. Shang, X.H. Xia, Visible-light-driven photocatalytic disinfection mechanism of Pb-$BiFeO_3$/rGO photocatalyst, Water Res. 161 (2019) 251–261, https://doi.org/10.1016/j.watres.2019.06.011.

[68] A.A. Ivanov, V. Gonzalez-Pecchi, L.F. Khuri, Q. Niu, Y. Wang, Y. Xu, Y. Bai, X. Mo, E.V. Prochownik, M.A. Johns, Y. Du, F.R. Khuri, H. Fu, OncoPPi-informed discovery of mitogen-activated protein kinase kinase 3 as a novel binding partner of c-Myc, Oncogene 36 (2017) 5852–5860, https://doi.org/10.1038/onc.2017.180.

[69] N.N. Belushkina, S.E. Severin, Molecular mechanisms of apoptosis pathology, Arkh. Patol. 63 (2001) 51–60.

[70] H. Li, H. Yang, D. Wang, L. Zhang, T. Ma, Peroxiredoxin2 (Prdx2) reduces oxidative stress and apoptosis of myocardial cells induced by acute myocardial infarction by inhibiting the TLR4/nuclear factor kappa B (NF-kB) signaling pathway, Med. Sci. Monitor 26 (2020) e926281.

[71] J.Y. Fang, C. Shang, Bromate formation from bromide oxidation by the UV/persulfate process, Environ. Sci. Technol. 46 (2012) 8976–8983, https://doi.org/10.1021/es300658u.

[72] Y.W. Xie, R.Y. Xu, R. Li, H.Y. Liu, J.P. Tian, L.J. Chen, Adsorbable organic halogens formed during treatment of Cl^- -containing wastewater by sulfate and hydroxyl radical-based advanced oxidation processes, Chem. Eng. J. 389 (2020), 124457, https://doi.org/10.1016/j.cej.2020.124457.

[73] J.R. Bolton, K.G. Bircher, W. Tumas, C.A. Tolman, Figures-of-merit for the technical development and application of advanced oxidation technologies for both electric- and solar-driven systems (IUPAC Technical Report), Pure Appl. Chem. 73 (2001) 627–637, https://doi.org/10.1351/pac200173040627.

[74] Y. Xu, Z.Y. Lin, H. Zhang, Mineralization of sucralose by UV-based advanced oxidation processes: UV/PDS versus UV/H_2O_2, Chem. Eng. J. 285 (2016) 392–401, https://doi.org/10.1016/j.cej.2015.09.091.

[75] C.S. Saavedra Sánchez, V.G. Álvarez Zavaleta, Conocimiento del sistema de tratamiento de agua de lastre Pureballast de Alfa Laval en los tripulantes de un buque tanque de la empresa naviera Elcano, (2021), http://repositorio.enamm.edu.pe/handle/ENAMM/175.